



Cite this: *Polym. Chem.*, 2025, **16**, 972

## Chemically recyclable poly(thioether-thioester)s via ring-opening polymerization of seven-membered thiolactones†

Long-Hai Liu, Si-Qi Wang, Hua-Zhong Fan, Qing Cao, Zhongzheng Cai \* and Jian-Bo Zhu \*

Developing new sulfur-containing polymers with chemical recyclability as next-generation high-performance sustainable polymeric materials is in high demand. Herein, we prepared two seven-membered thiolactone monomers (**M1** and **M2**) with sulfur incorporated at different positions. Both monomers displayed excellent reactivity towards ring-opening polymerization with >90% monomer conversion at room temperature. The resulting poly(thioether-thioester) products **P(M)**s exhibited high thermal stability and comparable mechanical properties ( $\sigma_B = \sim 30$  MPa,  $\varepsilon_B = \sim 660\%$ ) to commercial low-density polyethylene. Chemical recycling of **P(M1)** to its monomer **M1** could be accomplished with excellent yield and purity. Intriguingly, **P(M1)** could be applied for selective absorption and recovery of  $\text{Au}^{3+}$  with >99% efficiency by exploiting the chemical recyclability of **P(M1)**.

Received 17th December 2024,  
Accepted 15th January 2025  
DOI: 10.1039/d4py01442a  
[rsc.li/polymers](http://rsc.li/polymers)

## Introduction

The accumulation of petroleum-based plastic waste has caused serious environmental problems.<sup>1–4</sup> Currently, chemically recyclable polymers that are able to depolymerize back to their monomers under mild conditions have been developed as promising alternatives to traditional petroleum-based polymers.<sup>5–10</sup> The recent decade has witnessed significant breakthroughs in chemically recyclable polymers from polyesters to polyamides.<sup>11–24</sup> Monomer design represented an important strategy to manipulating the thermodynamics of the reversible ring-opening polymerization (ROP) and ring-closing depolymerization (RCD).<sup>25–28</sup> The development of new chemically recyclable polymers as next-generation sustainable polymeric materials is in high demand.

Sulfur-containing polymers have gained growing interest owing to their distinct merits such as outstanding optical and electrical characteristics and excellent adhesion to heavy metal ions.<sup>29–44</sup> As a result, sulfur-containing polymeric materials provide potential as engineering plastic, optical, photoelectronic, and heavy metal capture materials.<sup>43,45–47</sup> Consequently, developing a sulfur-containing polymer system with chemical

recyclability and outstanding properties would be significant and highly desired. To date, polythioesters and polydisulfides have been investigated as chemically recyclable polymers (Fig. 1).<sup>48</sup> These polythioesters illustrated stronger depolymerizability in comparison with their polyester analogues due to their elongated thioester bonds.<sup>49–57</sup> In addition, polydisulfides have been reported as elegant systems for chemical recycling to monomers.<sup>58–63</sup> Gutekunst and our group have reported a DTO monomer (1,4-dithian-2-one) as a facile platform to construct chemically recyclable poly(thioether-thioester)s.<sup>64,65</sup> However, this monomer suffered from low polymerization conversions at room temperature due to the low ring strain and its polymer product displayed poor thermal stability. To overcome these shortcomings, we proposed to construct seven-membered thiolactones owing to their enhanced ring strain. Herein, we have prepared two seven-membered-ring based monomers 1,4-dithiepan-2-one (**M1**) and 1,4-dithiepan-5-one (**M2**) and investigated their ROP performance with organic bases or **La** complexes as catalysts. The produced poly(thioether-thioester) **P(M)**s exhibited high air and thermal stability and distinct thermal and mechanical properties. **P(M2)** with sulfur incorporated at the 4 position exhibited a melting temperature ( $T_m$ ) of 95 °C and demonstrated high-performance mechanical properties ( $\sigma_B = 29.86 \pm 2.02$  MPa and  $\varepsilon_B = 663 \pm 60\%$ ). Notably, **P(M1)** with sulfur at the 5 position behaved as a soft material, which could be applied for selective absorption and recovery of  $\text{Au}^{3+}$  (>99% efficiency). Intriguingly, chemically recycling of **P(M1)** to the monomer could be carried out in solution or bulk with excellent yields, featuring a highly efficient recycling system.

National Engineering Laboratory of Eco-Friendly Polymeric Materials (Sichuan), College of Chemistry, Sichuan University, Chengdu 610064, People's Republic of China. E-mail: zzcai@scu.edu.cn, jbzhu@scu.edu.cn

† Electronic supplementary information (ESI) available. CCDC 2354510. For ESI and crystallographic data in CIF or other electronic format see DOI: <https://doi.org/10.1039/d4py01442a>

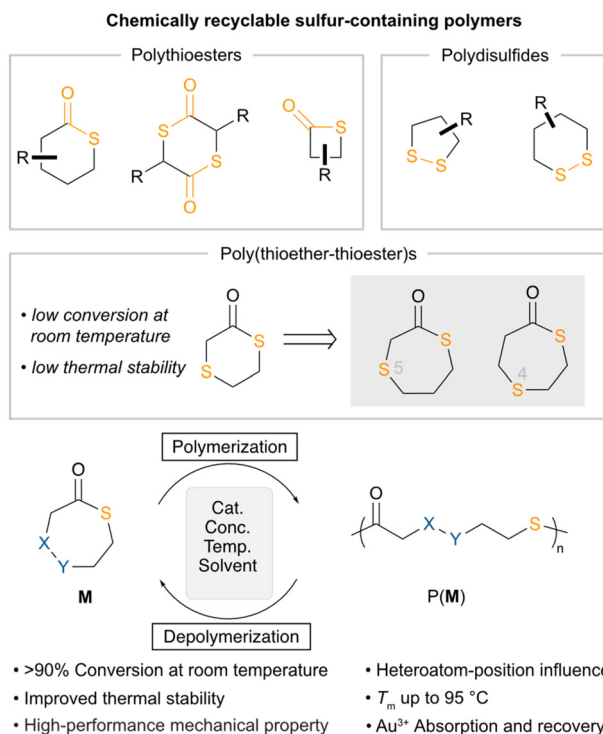


**Fig. 1** Representative chemically recyclable sulfur-containing polymers. Access to chemically recyclable seven-membered-based poly(thioether-thioester)s.

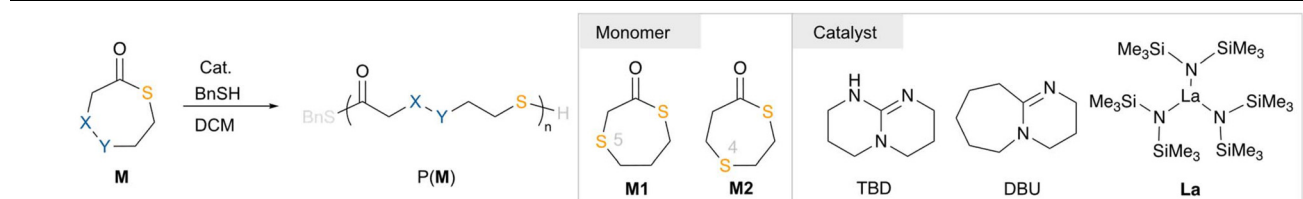
## Results and discussion

### Ring-opening polymerization

1,4-Dithiepan-2-one (**M1**) and 1,4-dithiepan-5-one (**M2**) were prepared according to a modified synthetic route.<sup>66</sup> 2.1 g of **M1** as colourless crystals was obtained *via* cyclization of 1,3-dimercaptopropane and chloroacetyl chloride in the presence of Et<sub>3</sub>N. Further scaling up of this synthetic procedure led to a significant decrease in monomer yield. **M2** was synthesized using a similar procedure except that 1,2-ethanedithiol and 3-chloropropionyl chloride were used as the starting materials. The <sup>1</sup>H NMR spectrum of **M1** was in a good agreement with a literature report.<sup>66</sup> For **M2**, its <sup>1</sup>H NMR spectrum was inconsistent with a previous report.<sup>67</sup> However, the accurate chemical structure of **M2** was confirmed by single-crystal X-ray diffraction analysis (Fig. S4†).

With these monomers in hand, the polymerization study of **M1** and **M2** was next carried out in DCM solution at room temperature with organic bases TBD, DBU, and **La** as catalysts and benzyl mercaptan (BnSH) as an initiator (Table 1). Among these catalysts, TBD acted as the most effective catalyst and promoted robust polymerization of **M1**, which reached >90% conversions within 10 min (Table 1, entries 1–4). Size exclusion chromatography (SEC) analysis revealed that increasing the [M1]:[TBD]:[BnSH] ratios from 100:1:1 to 1000:1:1 led to a gradual increase in *M<sub>n</sub>* from 8.8 to 62.1 kDa. These *M<sub>n</sub>* values were lower than the theoretical values (*M<sub>n,Calcd</sub>*) calculated from [M1]:[BnSH] ratios and monomer conversions. We believe that this is due to the inevitable chain transfer or the formation of a cyclic polymer. To verify our hypothesis, a P(**M1**) sample prepared with [M1]:[TBD]:[I] = 50:1:1 was

**Table 1** Ring-opening polymerization of **M1** and **M2**<sup>a</sup>



Entry	Monomer	Cat.	[M]/[Cat.]/[I]	Time (min)	Conv. <sup>b</sup> (%)	<i>M<sub>n,Calcd</sub></i> <sup>c</sup> (kg mol <sup>-1</sup> )	<i>M<sub>n</sub></i> <sup>d</sup> (kDa)	<i>D</i> <sup>d</sup>
1	<b>M1</b>	TBD	100:1:1	1	93	13.8	8.8	1.40
2	<b>M1</b>	TBD	200:1:1	1	93	27.5	13.7	1.41
3	<b>M1</b>	TBD	500:1:1	5	94	69.6	44.0	1.43
4	<b>M1</b>	TBD	1000:1:1	10	95	140.6	62.1	1.65
5	<b>M1</b>	DBU	500:1:1	60	73	54.0	33.9	1.92
6	<b>M1</b>	<b>La</b>	1000:1:0	180	17	—	18.7	1.84
7	<b>M1</b>	<b>La</b>	1000:1:3	180	12	5.9	24.7	1.51
8	<b>M2</b>	TBD	200:1:1	1	97	28.7	47.2 <sup>e</sup>	1.51 <sup>e</sup>
9	<b>M2</b>	TBD	500:1:1	10	98	72.5	101 <sup>e</sup>	1.55 <sup>e</sup>
10	<b>M2</b>	TBD	1000:1:1	60	97	144	220 <sup>e</sup>	1.56 <sup>e</sup>
11	<b>M2</b>	TBD	2000:1:1	120	77	228	256 <sup>e</sup>	1.62 <sup>e</sup>

<sup>a</sup> Conditions: [M] = 1.1 M, initiator (I) = benzyl mercaptan, RT. <sup>b</sup> Monomer conversion measured by <sup>1</sup>H NMR of the quenched solution.

<sup>c</sup> Calculated from  $[M]_0/[BnSH]_0 \times \text{Conv.} \times M_{\text{W}} + M_{\text{W}} \text{BnSH}$ . <sup>d</sup> Number-average molecular weight (*M<sub>n</sub>*) and dispersity index (*D* = *M<sub>w</sub>*/*M<sub>n</sub>*), determined by size exclusion chromatography (SEC) at 40 °C in THF. <sup>e</sup> Number-average molecular weight (*M<sub>n</sub>*) and dispersity index (*D* = *M<sub>w</sub>*/*M<sub>n</sub>*), determined by size exclusion chromatography (SEC) in DCM.

examined by matrix-assisted laser desorption ionization time-of-flight (MALDI-TOF) mass spectrometry. It displayed only one set of molecular ion peaks with the space between two neighbouring ion peaks being  $\sim 148$ , which is in good agreement with the molar mass of **M1**. Upon a linear fitting of the data, it showed an intercept of 22.98 which matched the molecular weight of  $\text{Na}^+(23.0)$ , confirming the presence of the cyclic structure of **P(M1)** (Fig. S32 $\dagger$ ). At a  $[\text{M1}]:[\text{DBU}]:[\text{BnSH}]$  ratio of 500 : 1 : 1, the polymerization approached 73% conversion within 60 min, delivering **P(M1)** with an  $M_n$  of 33.9 and a dispersity ( $D$ ) of 1.95 (Table 1, entry 5). Catalyst **La** displayed diminished activity with or without an alcohol initiator (Table 1, entries 6 and 7), presumably due to the stable coordination of thioether groups to the metal center, which further inhibited monomer insertion.

**M2** showed a similar reactivity pattern to **M1** and polymerized rapidly to achieve  $>95\%$  conversions with TBD as the catalyst (Table 1, entries 8–11). It should be noted that the resulting **P(M2)** products showed poor solubility in THF and their  $M_n$  values were then determined by SEC in a DCM eluent. With an increasing  $[\text{M2}]:[\text{TBD}]:[\text{BnSH}]$  ratio from 200 : 1 : 1 to 1000 : 1 : 1, the produced **P(M2)** exhibited a gradual growth in  $M_n$  from 47.2 to 220 kDa that was 1-fold higher than its corresponding theoretical value. We hypothesized that a poor correlation between relative molecular weights using polystyrene calibration and absolute molecular weights in these polar eluents could be responsible for the increased  $M_n$ . Notably, the polymerization of **M2** with an  $[\text{M2}]/[\text{TBD}]/[\text{I}]$  ratio of 2000/1/1 afforded **P(M2)** with an  $M_n$  of 256 kDa and a  $D$  of 1.62.

## Polymer characterization

To evaluate the thermal stability of these synthesized **P(M)** products, thermal gravimetric analysis (TGA) was first conducted. **P(M1)** and **P(M2)** demonstrated outstanding thermal stability with decomposition temperatures ( $T_d$ , defined as the temperature at 5% weight loss) of 293 and 275 °C, respectively (Fig. 2a). These values were significantly higher than those of previously reported chemically recyclable poly(thioether-thioester) **P(DTO)** ( $T_d = 227$  °C).<sup>65</sup> Next, the air stability was tested by placing **P(M1)** samples ( $M_n = 68.6$  kDa,  $D = 1.67$ ) inside an incubator at 25 °C, 40% relative humidity (RH) or 35 °C, 50% RH to monitor their weight and  $M_n$  changes over 5 weeks. As shown in Fig. 2b and c, the **P(M1)** sample exhibited negligible changes in  $M_n$  and  $D$  over 5 weeks. Moreover, these samples showed identical  $^1\text{H}$  NMR spectra to those of the pristine material after 5 weeks at 25 °C and 40% RH and 35 °C and 50% RH (Fig. S24 and S25 $\dagger$ ). These experiments underscored the excellent air and moisture stability of **P(M1)**.

Differential scanning calorimetry (DSC) was utilized to study the thermal properties of the **P(M)** product. **P(M1)** with sulfur incorporated at the 5 position displayed a near-room-temperature  $T_m$  of 47 °C on the first heating scan. This melting transition disappeared on the second heating scan and only a clear glass transition with a glass-transition temperature ( $T_g$ ) of  $-49$  °C was observed (Fig. 2d and e), suggesting a slow crystallization rate. In contrast, sulfur-incorporation at the 4 position contributed to a  $T_m$  of  $\sim 95$  °C on the first and second heating scans for **P(M2)**. The distinct crystallization

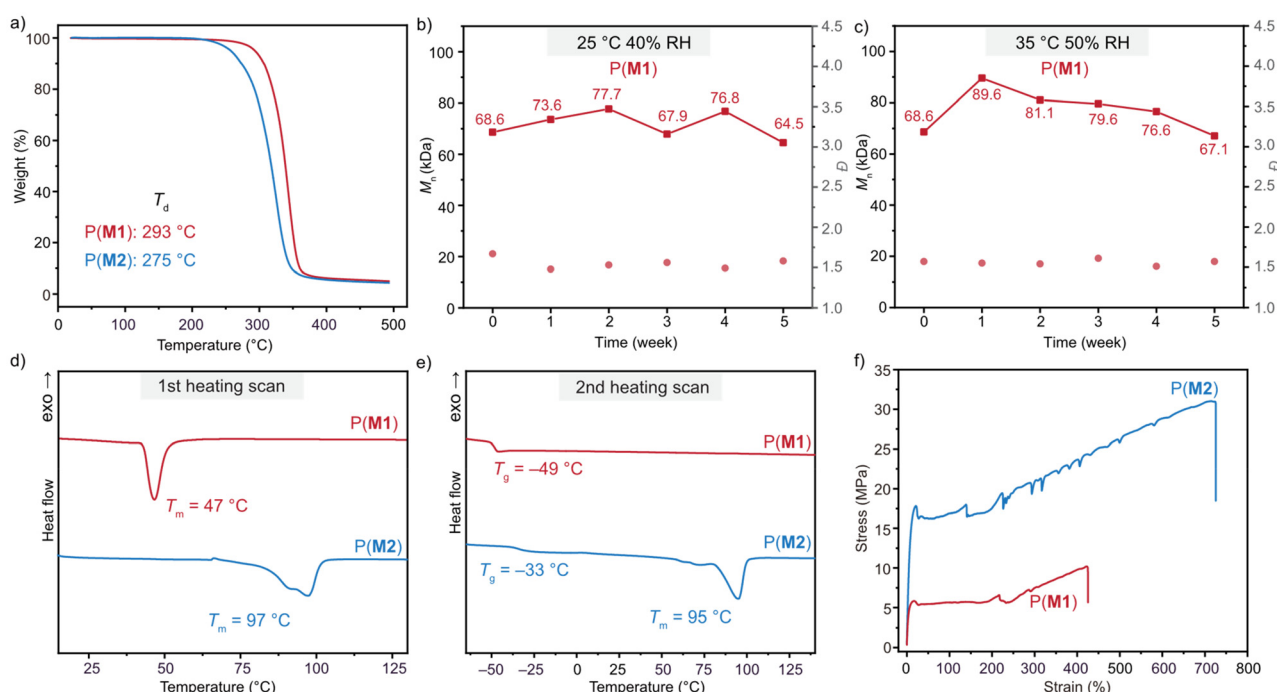


**Fig. 2** Polymer characterization. (a) TGA curves of **P(M)**s. (b) Humidity stability test of **P(M1)** at 25 °C, 40% RH. (c) Humidity stability test of **P(M1)** at 35 °C, 50% RH. (d) DSC curves of **P(M)**s on the first heating scan. (e) DSC curves of **P(M)**s on the second heating scan. (f) Strain–stress curves of **P(M)**s.

property between **P(M1)** and **P(M2)** illustrated the influence of the heteroatom incorporation position. Specifically, **P(M2)** with sulfur-incorporation at the 4 position adopted a more rigid and organized backbone structure, which resulted in an increased  $T_m$  and crystallization rate in comparison with those of **P(M1)**. Their semi-crystallinity was also confirmed by powder X-ray diffraction (PXRD) (Fig. S17 and S18†).

We next investigated the mechanical properties of **P(M1)** and **P(M2)** by tensile testing experiments. The dog-bone-shaped opaque **P(M1)** and **P(M2)** specimens were prepared by melt pressing at 50 °C and 110 °C, respectively. The formed **P(M)** films displayed similar  $M_n$  and  $D$  values with the original solid samples (Table S4†), indicative of no obvious degradation by hot pressing and further confirming the excellent thermal stability of **P(M1)** and **P(M2)**. Both **P(M1)** and **P(M2)** were subjected to uniaxial extension experiments at a strain rate of 10 mm min<sup>-1</sup> and exhibited distinct mechanical performance (Fig. 2f). **P(M1)** ( $M_n$  = 94.9 kDa,  $D$  = 1.56) containing an S atom at the 5 position showed a tensile strength at break ( $\sigma_B$ ) of 13.19 ± 1.45 MPa, an elongation at break ( $\varepsilon_B$ ) of 572 ± 45%, and a Young's modulus ( $E$ ) of 165 ± 8 MPa. In comparison with the soft **P(M1)**, **P(M2)** ( $M_n$  = 131.5 kDa,  $D$  = 2.08) exhibited both improved tensile strength and ductility, demonstrating  $\varepsilon_B$  = 29.86 ± 2.02 MPa,  $\varepsilon_B$  = 663 ± 60%, and  $E$  = 247 ± 28 MPa. These values were comparable to those of commercial low-density polyethylene (LDPE).<sup>21</sup>

### Chemical recycling to the monomer

To gain better understanding of the influence of the sulfur incorporation position on the chemical recyclability of the resulting polymers, we set out to calculate the thermodynamics of these two polymerization systems. Their ceiling temperature ( $T_c$ ) was determined by monitoring the polymerization equilibrium changes over a temperature range of 40 to 130 °C. Their standard-state thermodynamic parameters of  $\Delta H_p^\circ$  and  $\Delta S_p^\circ$  were calculated according to van't Hoff plots (Tables S7 and 8†). The thermodynamic parameters were calculated to be  $\Delta H_p^\circ = -8.24 \text{ kJ mol}^{-1}$  and  $\Delta S_p^\circ =$

$-10.49 \text{ J mol}^{-1} \text{ K}^{-1}$  for **P(M1)**. **P(M2)** demonstrated  $\Delta H_p^\circ = -20.79 \text{ kJ mol}^{-1}$  and  $\Delta S_p^\circ = -22.32 \text{ J mol}^{-1} \text{ K}^{-1}$ . Their relative  $T_c$  values at  $[\mathbf{M}]_0 = 1.0 \text{ M}$  for **P(M1)** and **P(M2)** were calculated to be 512 and 658 °C, respectively, manifesting the feasibility for depolymerizability. We inferred that the sulfur at the 5 position of **M1** could contribute to a more stable ring conformation, thereby delivering a lower  $T_c$  in comparison with **M2** having sulfur at the 4 position.

In line with our thermodynamic study, **P(M1)** underwent efficient chemical recycling to **M1** in the presence of 1 mol% of  $\text{Sn}(\text{Oct})_2$  at 150 °C, producing pure **M1** in 93% yield (Table S9†). To establish a close-loop economy of **P(M1)**, the recycled **M1** was treated with TBD and  $\text{BnSH}$  for repolymerization. To our delight, the recycled **M1** underwent repolymerization at  $[\mathbf{M1}]:[\text{TBD}]:[\text{I}]$  ratios of 100:1:1 and 500:1:1 without a decrease in polymerization reactivity, approaching 95% and 92% conversion within 10 min, respectively (Table S12†). These results highlighted the feasibility and efficiency of chemical recycling of **P(M1)** (Fig. 3).

Surprisingly, although various catalytic systems including  $t\text{-BuOK}$ ,  $\text{PhSNa}$ ,  $\text{Sn}(\text{Oct})_2$ ,  $\text{Sn}(\text{OAc})_2$ , **La**, and  $\text{Sb}_2\text{O}_3$  were screened for thermal bulk depolymerization of **P(M2)** at 100–175 °C (Table S10†), it was found that only 60% yield of **M2** could be collected from the depolymerization of **P(M2)** with  $\text{PhSNa}$  in 11 h at 170 °C. We speculated that it could be attributed to the poor polymer–catalyst contact effectiveness. Next, we examined the depolymerization of **P(M2)** in dilute solution (Table S11†). A 0.01 M solution of **P(M2)** at 160 °C with 5 mol%  $\text{Sn}(\text{OAc})_2$  converted back to **M2** in 62% yield in 11 h. Extending the depolymerization time led to no change in monomer recovery. Collectively, we inferred that the depolymerization of **P(M2)** was limited to the depolymerization kinetics.

### Application of **P(M1)** for $\text{Au}^{3+}$ absorption and recovery

Motivated by the excellent chemical recyclability of **P(M1)** and the presence of thioether groups in **P(M1)**, we speculated that it could be applied for  $\text{Au}^{3+}$  absorption and recovery. The

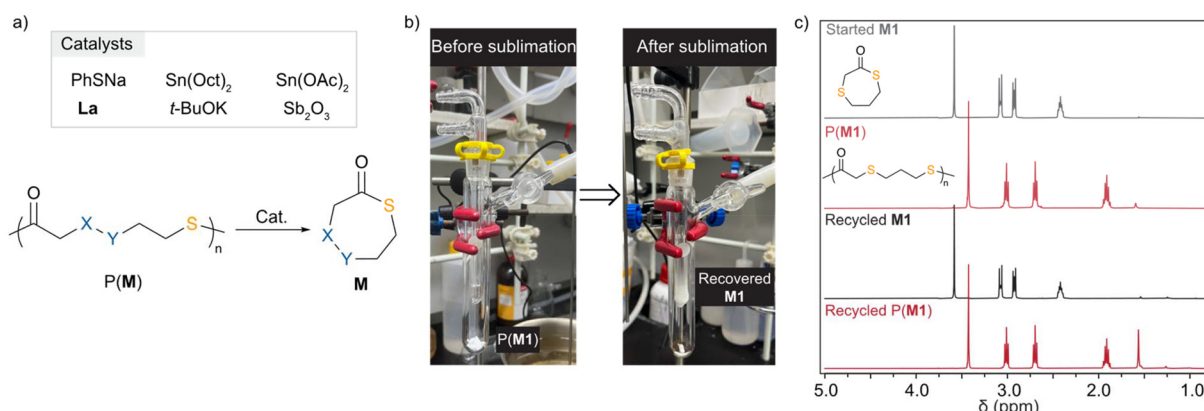


**Fig. 3** Chemical recycling of **P(M)**s. (a) Scheme for depolymerization. (b) The sublimation setup for the recycling of **P(M1)**. (c) <sup>1</sup>H NMR spectra of starting **M1**, **P(M1)**, recycled **M1**, and recycled **P(M1)**.

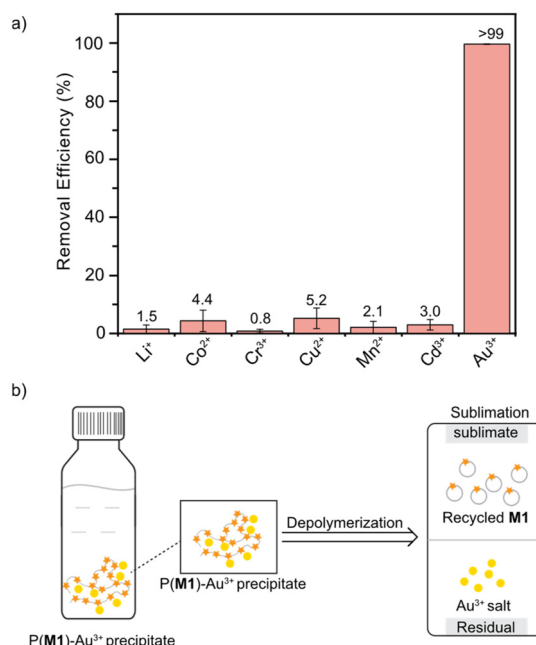


Fig. 4 Application of P(M1) for  $\text{Au}^{3+}$  absorption and recovery. (a) Metal ion removal efficiency of P(M1). (b) The diagram of the  $\text{Au}^{3+}$  absorption and recovery process.

sulphur atoms in the thioether groups readily form coordinate bonds with the empty d orbitals of metal ions because of their lone pair electrons, creating a strong electrostatic attraction. In a typical test, P(M1) (4 mg) dissolved in 100  $\mu\text{L}$  DCM was directly added into an aqueous solution containing  $\sim$ 60 ppm  $\text{Au}^{3+}$  (4 mL). After stirring for 2 h, the precipitated solid was separated by filtration. The atomic absorption spectroscopy (AAS) analysis of the remaining solution after filtration showed a >99% removal efficiency of  $\text{Au}^{3+}$  (Table S13† and Fig. 4a). In comparison, the adsorption of other metal ions such as  $\text{Co}^{2+}$ ,  $\text{Mn}^{2+}$ , and  $\text{Cu}^{2+}$  was almost negligible, which underlined the excellent adsorption selectivity of P(M1) for  $\text{Au}^{3+}$  over other metal ions. More importantly, P(M1) was able to accomplish the absorption and subsequent recovery process of  $\text{Au}^{3+}$  by the exploitation of its chemical recyclability. The P(M1) adsorbent after  $\text{Au}^{3+}$  adsorption was dried under vacuum and then transferred into a sublimation equipment. Sublimation was carried out at 140 °C under vacuum in the presence of  $\text{Sn}(\text{OAc})_2$  as the catalyst. M1 could be collected as the sublimate in 70–73% yields (Table S16 and Fig. S31†).  $^1\text{H}$  NMR analysis revealed the high purity of the recovered M1. Meanwhile, the left solid at the bottom of the sublimate contained the recovered  $\text{Au}^{3+}$ . This process revealed that P(M1) could serve as a promising chemically recyclable material for  $\text{Au}^{3+}$  adsorption and recovery.

## Experimental

### Materials and methods

All synthesis and manipulations of air- and moisture-sensitive materials were carried out in an argon-filled glovebox. All

reagents from Adamas-beta and Energy Chemical were used as received unless otherwise stated.

### $^1\text{H}$ NMR and $^{13}\text{C}$ NMR spectroscopy

$^1\text{H}$  and  $^{13}\text{C}$  NMR spectra were recorded on an Agilent 400-MR DD2 or a Bruker Advance 400 spectrometer ( $^1\text{H}$ : 400 MHz,  $^{13}\text{C}$ : 100 MHz). Chemical shifts ( $\delta$ ) for  $^1\text{H}$  and  $^{13}\text{C}$  NMR spectra are given in ppm relative to TMS. The residual solvent signals were used as references for  $^1\text{H}$  and  $^{13}\text{C}$  NMR spectra and the chemical shifts converted to the TMS scale ( $\text{CDCl}_3$ :  $\delta_{\text{H}} = 7.26$  ppm,  $\delta_{\text{C}} = 77.00$  ppm). The following abbreviations were used to explain the multiplicities: s = singlet, d = doublet, t = triplet, q = quartet, and m = multiplet. All spectra were processed with MestReNova 14.1.1 software, and coupling constants were reported as observed.

### Size exclusion chromatography (SEC)

Measurements of polymer absolute weight-average molecular weight ( $M_w$ ), number average molecular weight ( $M_n$ ), and molecular weight distributions or dispersity indices ( $D = M_w/M_n$ ) were performed *via* size exclusion chromatography (SEC). The SEC instrument consisted of an Agilent LC system equipped with one guard column and two PL gel 5  $\mu\text{m}$  mixed-C gel permeation columns and coupled with an Agilent G7162A 1260 Infinity II RI detector. The analysis was performed at 40 °C using THF as the eluent at a flow rate of 1.0 mL min<sup>-1</sup>. The instrument was calibrated with nine polystyrene standards, and chromatograms were processed with Agilent OpenLab CDS Acquisition 2.5 molecular weight characterization software.

### Differential scanning calorimetry (DSC)

The melting-transition temperature ( $T_m$ ) and glass-transition temperature ( $T_g$ ) of purified and thoroughly dried polymer samples were measured by differential scanning calorimetry (DSC) on a TRIOS DSC25, TA Instrument. All  $T_g$  values were obtained from a second scan after the thermal history was removed from the first scan.

### Thermo-gravimetric analysis (TGA)

The decomposition temperatures ( $T_d$ ) and maximum rate decomposition temperatures ( $T_{\max}$ ) of the polymers were measured by thermo-gravimetric analysis (TGA) on a TGA55 Analyzer, TA Instrument. The polymer samples were heated from ambient temperature to 500 °C at a heating rate of 10 °C min<sup>-1</sup>. The values of  $T_{\max}$  were obtained from derivative (wt% °C) vs. temperature (°C) plots and defined by the peak values, while  $T_d$  values were obtained from wt% vs. temperature (°C) plots and defined as the temperature at 5% weight loss.

### X-ray crystallographic analysis

Single crystal data were obtained using a Bruker D8 Venture single crystal X-ray diffractometer.

### Wide angle X-ray diffraction (WXRD)

Powder X-ray diffraction data were obtained using a Bruker D2 Phaser diffractometer with Cu-K $\alpha$  radiation ( $\lambda = 1.5416 \text{ \AA}$ ) at 30 kV and 10 mA (scan of  $2\theta = 1.5\text{--}60^\circ$  with a speed of  $1^\circ \text{ min}^{-1}$ ).

### Mechanical analysis

Tensile stress/strain testing was performed using an Instron 5967 universal testing system. Samples were made by melt press in a steel mold ( $50 \times 4 \times 0.4 \text{ mM}^2$ ) and were stretched at a strain rate of  $10 \text{ mm min}^{-1}$  at ambient temperature until break. The measurements were performed 4 times for each test, and the values reported are averaged from the measured data.

### Atomic absorption spectrometer (AAS)

AAS data were obtained using a VARIAN SpectrAA 220FS/220Z.

## Conclusions

In conclusion, we have prepared two seven-membered thiolactone monomers **M1** and **M2** with sulfur incorporated at 4 and 5 positions. The robust polymerization of these thiolactone monomers approached >90% conversion at room temperature, affording semicrystalline P(**M**) products with  $T_m$  values up to  $95^\circ\text{C}$ . These P(**M**) products exhibited high thermal stability ( $T_d$  up to  $293^\circ\text{C}$ ) and excellent air stability. P(**M1**) and P(**M2**) exhibited distinct mechanical properties. P(**M1**) represented a soft material while P(**M2**) illustrated superior tensile strength and ductility to LDPE. More importantly, P(**M1**) could efficiently and selectively convert back to **M1**, which underwent repolymerization to establish a closed-loop lifecycle. By exploiting the chemical recyclability, P(**M1**) showcased high efficiency capability for selective adsorption and recovery of  $\text{Au}^{3+}$ . Collectively, these poly(thioether-thioester)s based on the seven-membered thiolactones paved the pathway towards the development of next-generation chemically recyclable sulfur-containing polymers.

## Conflicts of interest

There are no conflicts to declare.

## Data availability

The data supporting this article have been included as part of the ESI.† Data are available upon reasonable request from the authors.

## Acknowledgements

This work was supported by the National Key R&D Program of China (2021YFA1501700), the National Natural Science Foundation of China (22071163, 22301197, and 22371194), and the Fundamental Research Funds from Sichuan University

(2023SCUNL103 and 2024SCUQJTX005). We would like to thank Peng-Chi Deng from the Analytical & Testing Center of Sichuan University as well as Dongyan Deng and Jing Li from the College of Chemistry at Sichuan University for compound testing.

## References

- 1 A. Stubbins, K. L. Law, S. E. Muñoz, T. S. Bianchi and L. Zhu, *Science*, 2021, **373**, 51–55.
- 2 G. Hole and A. S. Hole, *Sustainable Prod. Consum.*, 2020, **23**, 42–51.
- 3 F. Zhang, F. Wang, X. Wei, Y. Yang, S. Xu, D. Deng and Y.-Z. Wang, *J. Energy Chem.*, 2022, **69**, 369–388.
- 4 J. M. Garcia and M. L. Robertson, *Science*, 2017, **358**, 870–872.
- 5 G. W. Coates and Y. D. Y. L. Getzler, *Nat. Rev. Mater.*, 2020, **5**, 501–516.
- 6 X.-L. Li, K. Ma, F. Xu and T.-Q. Xu, *Chem. – Asian J.*, 2023, **18**, e202201167.
- 7 C. M. Plummer, L. Li and Y. Chen, *Macromolecules*, 2023, **56**, 731–750.
- 8 Y. Sun, Z. An, Y. Gao, R. Hu, Y. Liu, H. Lu, X.-B. Lu, X. Pang, A. Qin, Y. Shen, Y. Tao, Y.-Z. Wang, J. Wang, G. Wu, G.-P. Wu, T.-Q. Xu, X.-H. Zhang, Y. Zhang, Z. Zhang, J.-B. Zhu, M. Hong and Z. Li, *Sci. China: Chem.*, 2024, **67**, 2803–2841.
- 9 S. Yang, S. Du, J. Zhu and S. Ma, *Chem. Soc. Rev.*, 2024, **53**, 9609–9651.
- 10 C. Shi, E. C. Quinn, W. T. Diment and E. Y.-X. Chen, *Chem. Rev.*, 2024, **124**, 4393–4478.
- 11 M. Hong and E. Y.-X. Chen, *Nat. Chem.*, 2016, **8**, 42–49.
- 12 J.-B. Zhu, E. M. Watson, J. Tang and E. Y.-X. Chen, *Science*, 2018, **360**, 398–403.
- 13 R. M. Rapagnani, R. J. Dunscomb, A. A. Fresh and I. A. Tonks, *Nat. Chem.*, 2022, **14**, 877–883.
- 14 Y.-T. Yan, G. Wu, S.-C. Chen and Y.-Z. Wang, *Sci. China: Chem.*, 2022, **65**, 943–953.
- 15 C. Li, L. Wang, Q. Yan, F. Liu, Y. Shen and Z. Li, *Angew. Chem., Int. Ed.*, 2022, **61**, e202201407.
- 16 Y.-M. Tu, X.-M. Wang, X. Yang, H.-Z. Fan, F.-L. Gong, Z. Cai and J.-B. Zhu, *J. Am. Chem. Soc.*, 2021, **143**, 20591–20597.
- 17 L. Wursthorn, K. Beckett, J. O. Rothbaum, R. M. Cywar, C. Lincoln, Y. Kratish and T. J. Marks, *Angew. Chem., Int. Ed.*, 2023, **62**, e202212543.
- 18 L. Ye, X. Liu, K. B. Beckett, J. O. Rothbaum, C. Lincoln, L. J. Broadbelt, Y. Kratish and T. J. Marks, *Chem.*, 2024, **10**, 172–189.
- 19 W. Zhang, J. Dai, Y.-C. Wu, J.-X. Chen, S.-Y. Shan, Z. Cai and J.-B. Zhu, *ACS Macro Lett.*, 2022, **11**, 173–178.
- 20 H. Chen, Z. Shi, T.-G. Hsu and J. Wang, *Angew. Chem., Int. Ed.*, 2021, **60**, 25493–25498.
- 21 B. A. Abel, R. L. Snyder and G. W. Coates, *Science*, 2021, **373**, 783–789.
- 22 C. Shi, W. Diment and E. Y.-X. Chen, *Angew. Chem., Int. Ed.*, 2024, e202405083.

23 Q. Cao, Y.-M. Tu, H.-Z. Fan, S.-Y. Shan, Z. Cai and J.-B. Zhu, *Angew. Chem., Int. Ed.*, 2024, **63**, e202400196.

24 D. Sathe, S. Yoon, Z. Wang, H. Chen and J. Wang, *Chem. Rev.*, 2024, **124**, 7007–7044.

25 C. Shi, Z.-C. Li, L. Caporaso, L. Cavallo, L. Falivene and E. Y.-X. Chen, *Chem.*, 2021, **7**, 670–685.

26 Y.-M. Tu, F.-L. Gong, Y.-C. Wu, Z. Cai and J.-B. Zhu, *Nat. Commun.*, 2023, **14**, 3198.

27 J. Zhou, D. Sathe and J. Wang, *J. Am. Chem. Soc.*, 2022, **144**, 928–934.

28 Z. Cai, Y. Liu, Y. Tao and J.-B. Zhu, *Acta Chim. Sin.*, 2022, **80**, 1165–1182.

29 A. Kausar, S. Zulfiqar and M. I. Sarwar, *Polym. Rev.*, 2014, **54**, 185–267.

30 H. Li, S. M. Guillaume and J.-F. Carpentier, *Chem. – Asian J.*, 2022, **17**, e202200641.

31 C.-J. Zhang, T.-C. Zhu, X.-H. Cao, X. Hong and X.-H. Zhang, *J. Am. Chem. Soc.*, 2019, **141**, 5490–5496.

32 W. Xiong, J. Dai, Z. Cai and J.-B. Zhu, *Polymer*, 2024, **290**, 126515.

33 K. Li, J.-L. Cheng, M.-Y. Wang, W. Xiong, H.-Y. Huang, L.-W. Feng, Z. Cai and J.-B. Zhu, *Angew. Chem., Int. Ed.*, 2024, **63**, e202405382.

34 H.-Z. Fan, X. Yang, J.-H. Chen, Y.-M. Tu, Z. Cai and J.-B. Zhu, *Angew. Chem., Int. Ed.*, 2022, **61**, e202117639.

35 J. M. M. Pople, T. P. Nicholls, L. N. Pham, W. M. Bloch, L. S. Lisboa, M. V. Perkins, C. T. Gibson, M. L. Coote, Z. Jia and J. M. Chalker, *J. Am. Chem. Soc.*, 2023, **145**, 11798–11810.

36 S. Wang, Z.-Y. Tian and H. Lu, *Angew. Chem., Int. Ed.*, 2024, **63**, e202411630.

37 T. Lee, P. T. Dirlam, J. T. Njardarson, R. S. Glass and J. Pyun, *J. Am. Chem. Soc.*, 2022, **144**, 5–22.

38 T. S. Kleine, N. A. Nguyen, L. E. Anderson, S. Namnabat, E. A. Lavilla, S. A. Showghi, P. T. Dirlam, C. B. Arrington, M. S. Manchester, J. Schwiegerling, R. S. Glass, K. Char, R. A. Norwood, M. E. Mackay and J. Pyun, *ACS Macro Lett.*, 2016, **5**, 1152–1156.

39 W. J. Chung, J. J. Griebel, E. T. Kim, H. Yoon, A. G. Simmonds, H. J. Ji, P. T. Dirlam, R. S. Glass, J. J. Wie, N. A. Nguyen, B. W. Guralnick, J. Park, Á. Somogyi, P. Theato, M. E. Mackay, Y.-E. Sung, K. Char and J. Pyun, *Nat. Chem.*, 2013, **5**, 518–524.

40 T.-J. Yue, L.-Y. Wang and W.-M. Ren, *Polym. Chem.*, 2021, **12**, 6650–6666.

41 X.-F. Zhu, G.-W. Yang, R. Xie and G.-P. Wu, *Angew. Chem., Int. Ed.*, 2022, **61**, e202115189.

42 A. L. Speelman, I. Čorić, C. Van Stappen, S. DeBeer, B. Q. Mercado and P. L. Holland, *J. Am. Chem. Soc.*, 2019, **141**, 13148–13157.

43 Y. Sun, C. Zhang and X. Zhang, *Chem. – Eur. J.*, 2024, **30**, e202401684.

44 T.-J. Yue, W.-M. Ren and X.-B. Lu, *Chem. Rev.*, 2023, **123**, 14038–14083.

45 J.-Z. Zhao, T.-J. Yue, B.-H. Ren, X.-B. Lu and W.-M. Ren, *Nat. Commun.*, 2024, **15**, 3002.

46 W. Cao, F. Dai, R. Hu and B. Z. Tang, *J. Am. Chem. Soc.*, 2020, **142**, 978–986.

47 T. Tian, R. Hu and B. Z. Tang, *J. Am. Chem. Soc.*, 2018, **140**, 6156–6163.

48 W. Xiong and H. Lu, *Sci. China: Chem.*, 2023, **66**, 725–738.

49 C. Shi, M. L. McGraw, Z. C. Li, L. Cavallo, L. Falivene and E. Y. X. Chen, *Sci. Adv.*, 2020, **6**, 1–12.

50 Y.-T. Guo, C. Shi, T.-Y. Du, X.-Y. Cheng, F.-S. Du and Z.-C. Li, *Macromolecules*, 2022, **55**, 4000–4010.

51 M. Wang, Z. Ding, X. Shi, Z. Ma, B. Wang and Y. Li, *Macromolecules*, 2024, **57**, 869–879.

52 Y. Wang, M. Li, J. Chen, Y. Tao and X. Wang, *Angew. Chem., Int. Ed.*, 2021, **60**, 22547–22553.

53 J. Yuan, W. Xiong, X. Zhou, Y. Zhang, D. Shi, Z. Li and H. Lu, *J. Am. Chem. Soc.*, 2019, **141**, 4928–4935.

54 W. Xiong, W. Chang, D. Shi, L. Yang, Z. Tian, H. Wang, Z. Zhang, X. Zhou, E.-Q. Chen and H. Lu, *Chem.*, 2020, **6**, 1831–1843.

55 D. Zhang, X. Wang, Z. Zhang and N. Hadjichristidis, *Angew. Chem., Int. Ed.*, 2024, **63**, e202402233.

56 L. Zhou, L. T. Reilly, C. Shi, E. C. Quinn and E. Y.-X. Chen, *Nat. Chem.*, 2024, **16**, 1357–1365.

57 P. Yuan, Y. Sun, X. Xu, Y. Luo and M. Hong, *Nat. Chem.*, 2022, **14**, 294–303.

58 Q. Zhang, Y. Deng, C.-Y. Shi, B. L. Feringa, H. Tian and D.-H. Qu, *Matter*, 2021, **4**, 1352–1364.

59 Q. Zhang, C.-Y. Shi, D.-H. Qu, Y.-T. Long, B. L. Feringa and H. Tian, *Sci. Adv.*, 2022, **4**, eaat8192.

60 W. Zou, J. Dong, Y. Luo, Q. Zhao and T. Xie, *Adv. Mater.*, 2017, **29**, 1606100.

61 X. Zhang and R. M. Waymouth, *J. Am. Chem. Soc.*, 2017, **139**, 3822–3833.

62 Y. Liu, Y. Jia, Q. Wu and J. S. Moore, *J. Am. Chem. Soc.*, 2019, **141**, 17075–17080.

63 S. Pal, A. Sommerfeldt, M. B. Davidsen, M. Hinge, S. U. Pedersen and K. Daasbjerg, *Macromolecules*, 2020, **53**, 4685–4691.

64 K. A. Stellmach, M. K. Paul, M. Xu, Y.-L. Su, L. Fu, A. R. Toland, H. Tran, L. Chen, R. Ramprasad and W. R. Gutekunst, *ACS Macro Lett.*, 2022, **11**, 895–901.

65 J. Dai, W. Xiong, M.-R. Du, G. Wu, Z. Cai and J.-B. Zhu, *Sci. China: Chem.*, 2023, **66**, 251–258.

66 C. M. Archer, J. R. Dilworth, D. V. Griffiths, M. J. Al-Jeboori, J. D. Kelly, C. Lu, M. J. Rosser and Y. Zheng, *J. Chem. Soc., Dalton Trans.*, 1997, 1403–1410.

67 Z. Xiao, Y. Wang, X. Chen, J. Long and Z. Wei, *J. Chem. Sci.*, 2017, **129**, 1595–1601.